Computer-AidedDesign

Taylor & Francis
Taylor & Francis Group

Image analysis using recurrence quantification plots, surface modeling and fused deposition modeling tools to design 3 dimensional models

R. Jill Urbanic

University of Windsor, Canada

ABSTRACT

Recurrence quantification analysis is a data analysis tool employed to visualise dynamic, non-linear, noisy data. This tool produces graphical displays for systems that have inherently non-predictable behavior. The graphical displays to explore system characteristics are 2D, and may use color coding to represent certain conditions. A method to create 3D results, and dynamic RQ plot visualization via rapid prototyping tool path visualization tools, is presented in this research. The inputs are linear data series created from digital image position and pixel color pairs. This 3D model introduces an additional mode to evaluate recurrence quantification results, and provides a platform for employing Boolean analysis to explore additional insights.

1. Introduction

Many 'time-series' data analysis strategies are available to extract information from a data set. Various strategies can be applied to filter out noise in order to estimate underlying trends; or transformations such as analysing the data in the frequency domain or phase space [6] could be performed to provide insights into a dynamic system. Recurrence quantification analysis (RQA) is a non-linear data analysis tool and was developed to visualise recurrence behaviors [14, 15]. Recurrence plots (RPs) are N x N matrix based representations formulated by:

$$RP_{i,j} = \Theta(\varepsilon - \| \overrightarrow{x_i} - \overrightarrow{x_j} \|) \qquad (1.1)$$

where $i, j = 1$ to N $\overrightarrow{x_i}$ is the point in phase space at which the system is situated at time i,

ϵ is a predefined threshold, and

$\Theta(x)$ is the Heaviside function.

The input parameters for the analysis are the:

- Data series
- Embedding value
- Delay period value
- First point within the sequence to start the analysis
- Last point or N
- Threshold for filtering (or Radius)

For a 'true condition', the grid element (i, j) is encoded black, else it remains white. The recurrence plot for a normalized sine wave with 8 periods within the data set is illustrated in Fig. 1. The sine wave was generated using the Grasshopper© Graph Mapper tool. Grasshopper© is a graphical algorithm editor [5] which has been designed to integrate with Rhinoceros© computer aided design (CAD) modeling tools [7]. There are modules for manipulating curves, surfaces, vectors, data sets, and the resulting image color, textures, and shadows. The RQ plot is generated using Python script [4] for Grasshopper© along with geometry creation tools, and the data is displayed using Rhinoceros©. After the points are created, boxes are generated around each point (Fig. 1 (a)), and then bounded surfaces are created (Fig. 1 (b)).

RQA has been performed in a diverse array of fields, including behavior sciences [1, 13–15], advanced manufacturing [3], gas-solid fluidized beds [9], and climate change influences [16]. There are common characteristics for these research areas at the abstract level: these systems are dynamic, non-linear, noisy, and unpredictable. Patterns within the observational data may not be readily evident. In addition to utilizing RQA to highlight recurrence patterns, the influence of noise within the observational data is studied [10] as the noise impacts the information being plotted. However, as recognized by Webber and Zbilut [13], RQ plots are "intriguing graphical displays" and "tend more to evoke artistic than scientific appreciation". The resulting RQ plots from the various areas of research are visually intriguing; therefore, goal of this research is to explore recurrences in a signal (digital image color or gray scale values), and

---

CONTACT R. Jill Urbanic ✉ jurbanic@uwindsor.ca
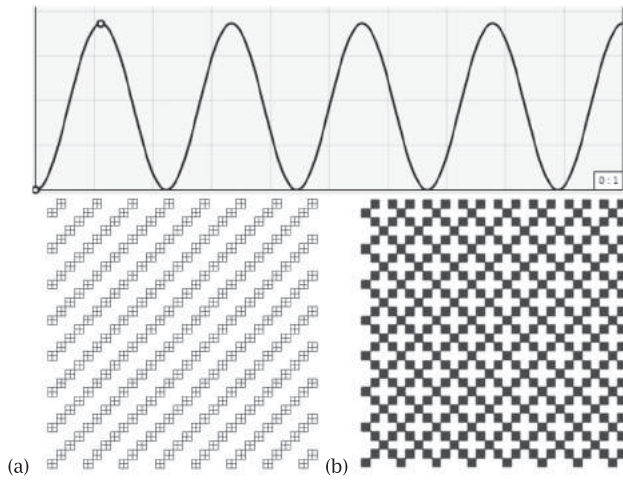
Figure 1. Sine wave and the resulting RP showing the points, boundaries, and grids (a) embedding = 5, delay = 5, first point = 0, last point = 30, Radius = 5, (b) embedding = 5, delay = 8, first point = 0, last point = 30, Radius = 5.

create a three dimensional (3D) model of the results so quantifiable analyses can be performed. Creating a 3D model would provide additional insights, and allow data to be partitioned or scenarios directly compared. Along with using the aforementioned computer aided design (CAD) modeling tools, Stratasys Insight© software [8], used for fused deposition modeling (FDM) process planning, is employed to create 'slice models' for dynamic visualization. Being able to dynamically change the RQA characteristics and visualize the results in 3D may provide more relevant and quantifiable pattern recognition insights.

An overview of the RQA parameters and equations is presented next, with some simple examples. The methodology utilized to create the input data set, develop the 2D and 3D models, and develop a 'sliced model' is explained in section 2.0. The results for traditional grid based plots and 3D plots are presented in section 3.0 for a variety of images. The summary is presented section 4.0.

1.1. Recurrence quantification analysis overview

RQA was first introduced by Eckmann et al. [2] as a graphical, qualitative technique to be able to interpret characteristics within dynamic systems, and highlight features that were otherwise inaccessible. A state recurs if it has neighbours in the phase space [12]. There are seven constant parameters that can be adjusted as required, which control the plot size, texture, and scaling. The embedding value is the vector dimension in which the dynamic should be projected, as shown here:

$$V_i = P_i + P_{i+delay} + P_{i+delay*2} + \cdots + P_{i+delay(embed-1)}$$
$$(1.2)$$

Where P_i is the data value for the ith point, and i is the starting point within the series,

V_i is the ith vector to be analysed, and

i indexes from i to $N+i$

The delay between sequential points should be selected to minimize the interaction between points of the measured series. The embed and delay parameters are illustrated in Fig. 2.

The third parameter is N, the range, which is defined by selecting the first and last points within the series. There are three methods in representing the 'norm' (fourth) recurrence parameter: the minimum, maximum norm, and Euclidean norms. The Euclidean norm is
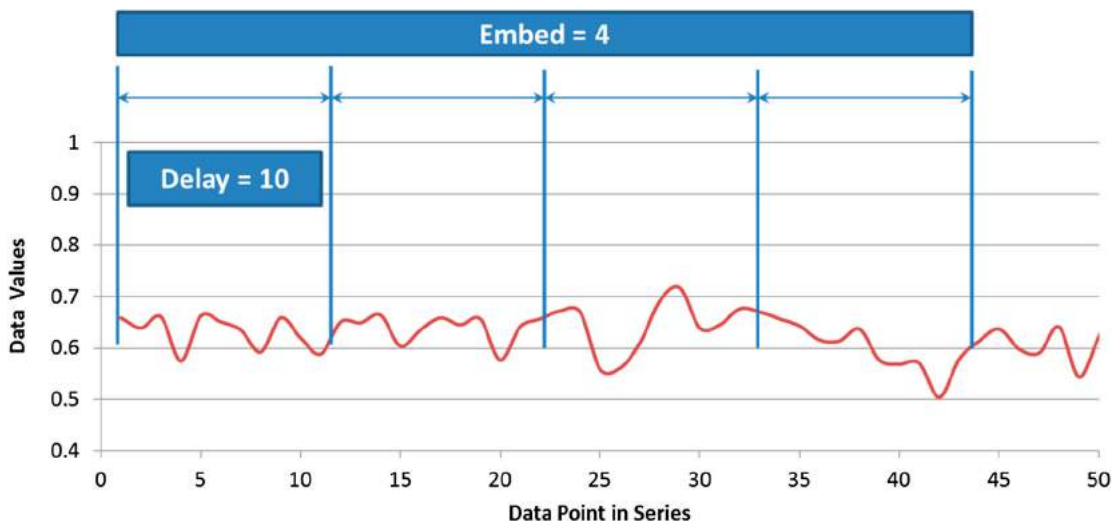
Figure 2. Random data series illustrating the delay parameter and the embedding parameter.
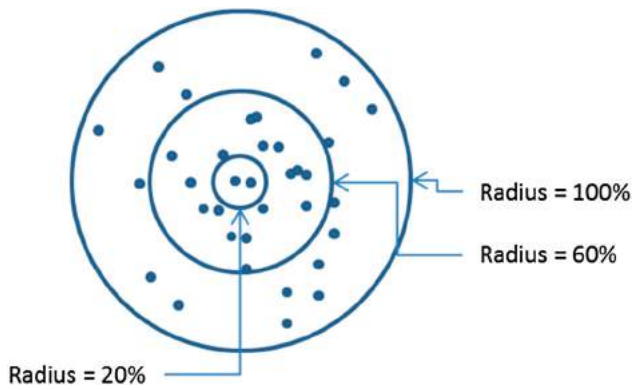
Figure 3. Phase space representation for a normalized Radius percentage. The points falling within the smallest circle are the nearest neighbours to that reference value. Increasing the reference value (larger concentric circle) increases the amount of points (adapted from [13]).

employed in this work, and is defined by:

$$Euclidean\ distance = \sum_{i=1}^{I}\sum_{j=1}^{J}\sqrt[2]{(V_i - V_j)^2} \qquad (1.3)$$

The fifth recurrence parameter is a scaling parameter. In this work, the calculated values are normalized to the maximum values, and then scaled to create height texture on the 3D model. The threshold, or Radius, is the sixth recurrence parameter, and is essentially a cut off parameter (Fig. 3). Using a 3D approach, and FDM slicing software, enables a dynamic visualization of all threshold values, the granularity of which is defined by the model slices.

The last parameter (not used in this work) is a line length filter. If a recurrence feature line length is less than this parameter, it is not plotted.

1.2. Super-imposed sine wave examples

Harmonic curves are presented to illustrate RQ plots for various parameters (Figs. 4–7). Low frequency and higher frequency superimposed sine waves are used as
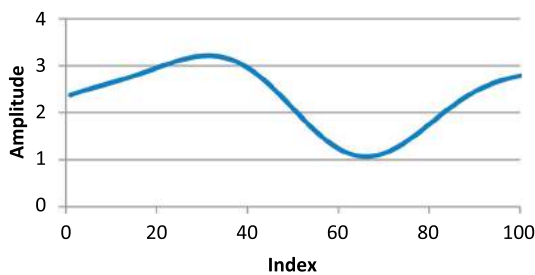
Figure 4. 100 of 1200 data series points used for the RQA analyses and plots illustrated in Fig. 5.
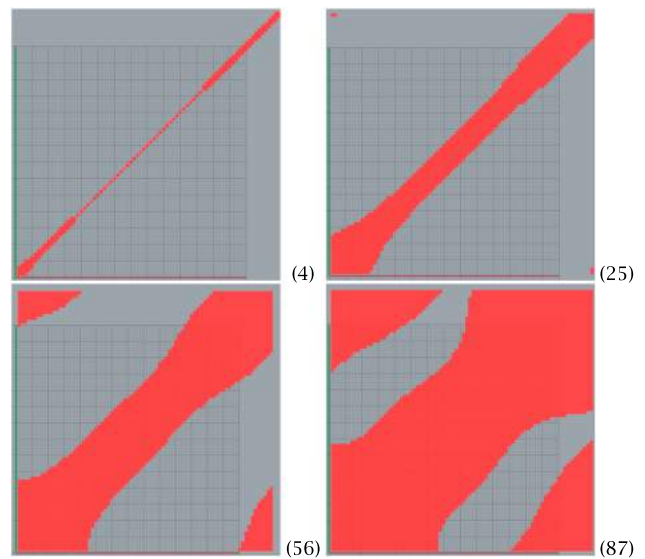
Figure 5. RQ plots for the sine wave based data series (embed = 5, delay = 8, Last point = 80, Radius value as noted.
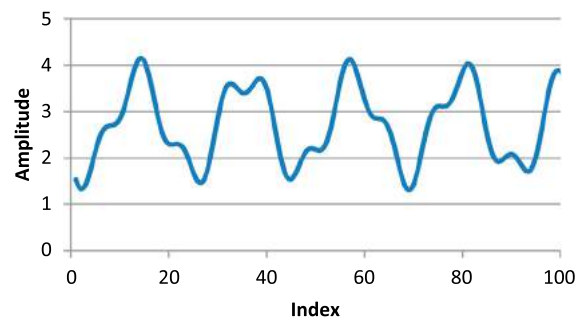
Figure 6. 100 of 1200 data series points used for the RQA analyses and plots illustrated in Fig. 7.
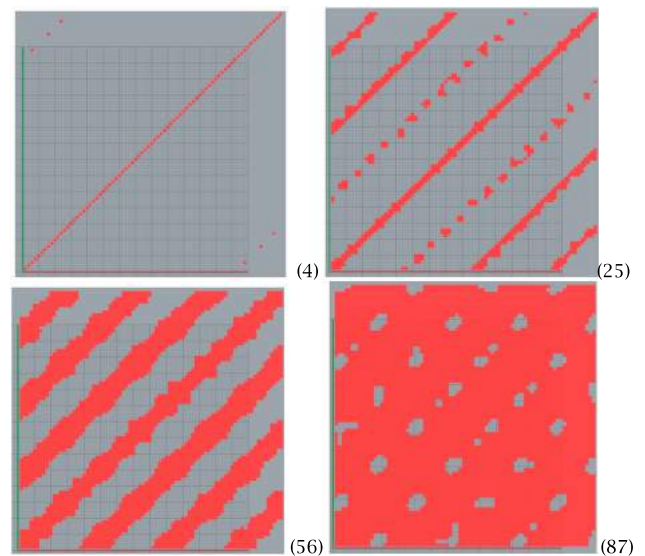
Figure 7. RQ plots for the sine wave based data series (embed = 5, delay = 8, Last point = 80, Radius value as noted.

the raw input data. The results are plotted for various Radius values that vary between 1–100 percent for these models. The series periodicity characteristics are evident in the plots. Note the default color values for geometry created in Rhinoceros© is red, and the background is gray; hence, the color representation in the balance of the figures.

Researchers have used color representation to illustrate various threshold values in lieu of the binary Heaviside function. This is also interesting, but a 'textured' 3D model will generate another level of information. Instead of a time series based input, a digital image file is flattened into linearized data series, 3D RQ plots generated, and saved in a format that allows physical

Create a data series
- Decompose pixel positions and values into a flat list
- x axis: pixel counter
- y axis vector value of the colour

Perform RQA
- Select parameters (embed, delay, last point, radius)
- Calculate Euclidean normal
- Filter the results (via the radius value)

Plot the results
- Create a bounded rectangle around each filtered point in the grid
- Create a surface within the bounded rectangle

Create 3D model
- Create an extrusion path vector based on the Euclidean Norm values
- Extrude the bounded rectangle by the vector

Save file in the *.STL format
- Validate *.stl mesh model is water tight

Develop a fabrication plan using the FDM software
- Create a dynamic RQ plot set

Figure 8. General process flow summary.

Figure 9. RQ plot Grasshopper© program illustrating the input data series, and the RQ inputs into a Python script which can be modified by the user for real time result updates.

Figure 10. Data acquisition: (a) Image data file to sample point set, (b) screen shot of a Mobius strip solid model with through holes, (c) a French curve (with reflection noise), (d) an Ammonite, and (e) a ginger cat.
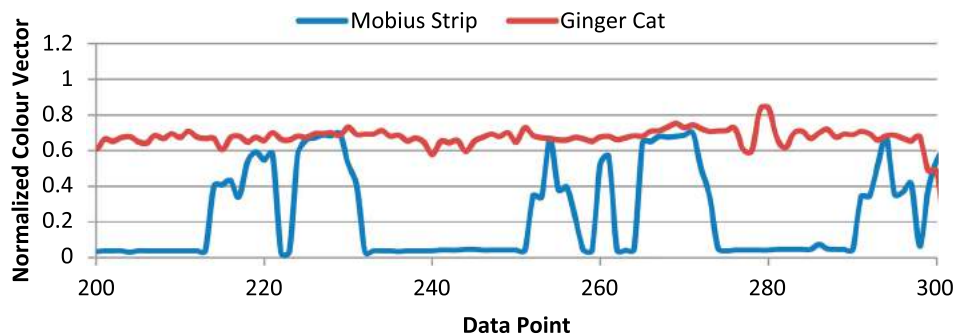
Figure 11. 100 data points from the flat series created from two digital images.

fabrication techniques to be performed. The methodology is described in the next section.

2. Methodology

A six step methodology is utilized to develop a 3D model of RQ plots: (i) data acquisition, (ii) RQ analysis, (iii) plotting the results using CAD primitives (points, curves, and surfaces), (iv) creating a 3D model, (v) creating a mesh model that can be utilized by additive

manufacturing process planning software, and (vi) using the additive manufacturing process planning software to create a 'slice' model to dynamically view all threshold results (Fig. 8). The general graphical algorithm developed for this work (in Grasshopper) is shown in Fig. 9.

The data series is modified to use a decomposed digital image as the input 'rawSeries'. The input values can be adjusted dynamically by positioning the cursor over the '◊' symbol, and dragging the slider bar between the
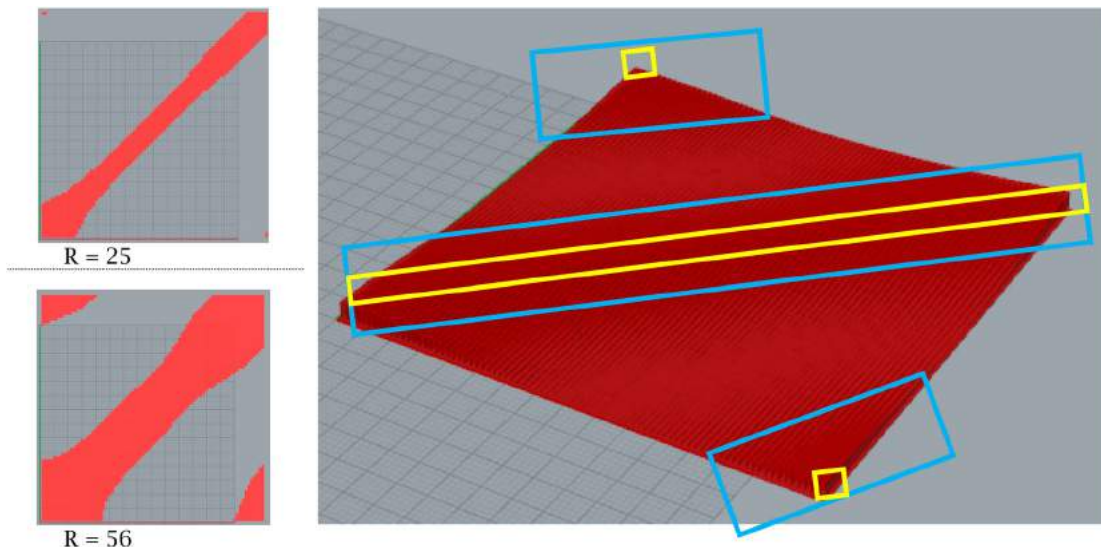
Figure 12. 3D RQ plot for the conditions illustrated in 4 and 5, where the yellow box approximates R = 25, and the blue approximates R = 56.
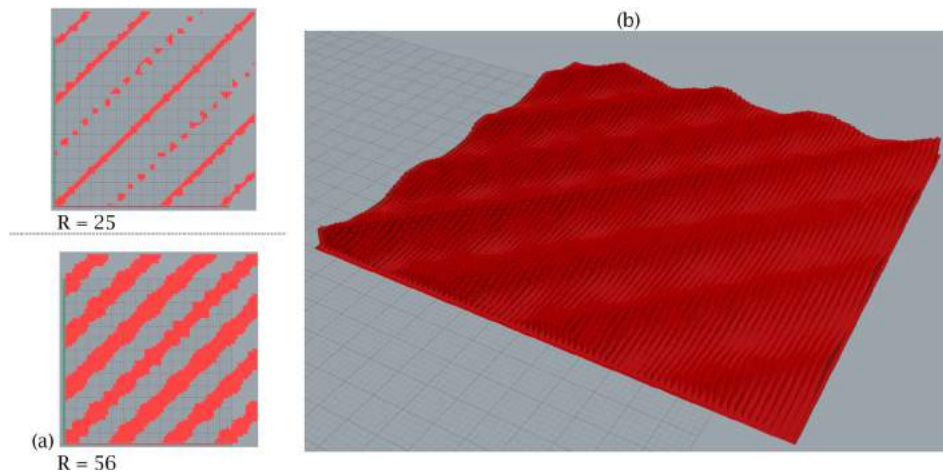
Figure 13. 3D RQ plot for the conditions illustrated in 6 and 7.
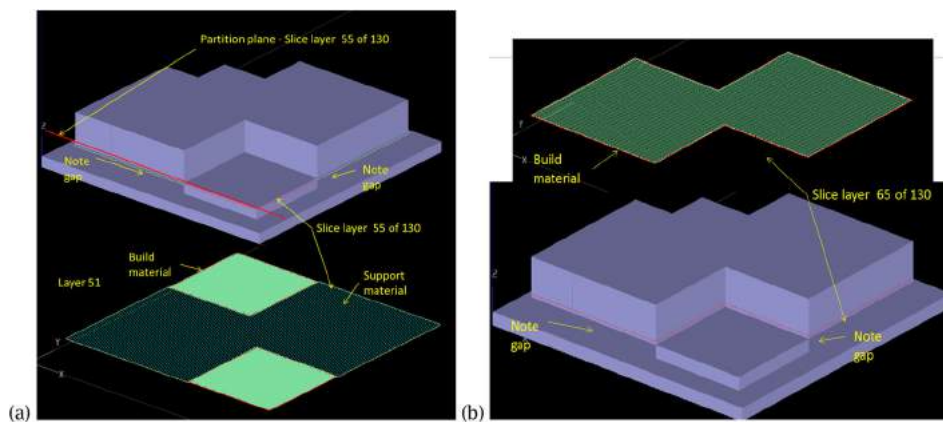
Figure 14. RQ 3D model plot of a Mobius Strip (embed = 7, Delay = 9, Last Point = 10).

Note: for illustration purposes, an *XY* reference plane is established at Radius = 25, and geometry which does not meet the threshold is extruded in the −z direction, and geometry which meets the threshold is extruded in the + z direction. This generates a physical gap in the model, which requires support material for fabrication (Fig. 14 a). Fig. 14 (b) shows a typical slice (boundary and fill).

(a)

(b)

(c)

Radius decreasing: R = 87, 56, 25, 4

Mobius strip: **embed = 10**, **Delay = 5**, Last Point = 40, Radius = (**variable**)

Mobius strip: embed = 10, **Delay = 9**, Last Point = 40, Radius = (**variable**)

Mobius strip: **embed = 7, Delay = 9**, Last Point = 40, Radius = (**variable**)

Radius decreasing: R = 56, 25, 4

Mobius strip: embed = 7, Delay = 9, Last Point = 120, Radius = (**variable**), and overlay of
Mobius strip plots: embed = 7, Delay = 9, **Last Point = 120**, Radius 25 (red) Radius = 56(black).

Figure 15. (a) Mobius strip, (b) partial data signal, and (c) RQ plots with parameter sets as labeled showing the input variable impact.
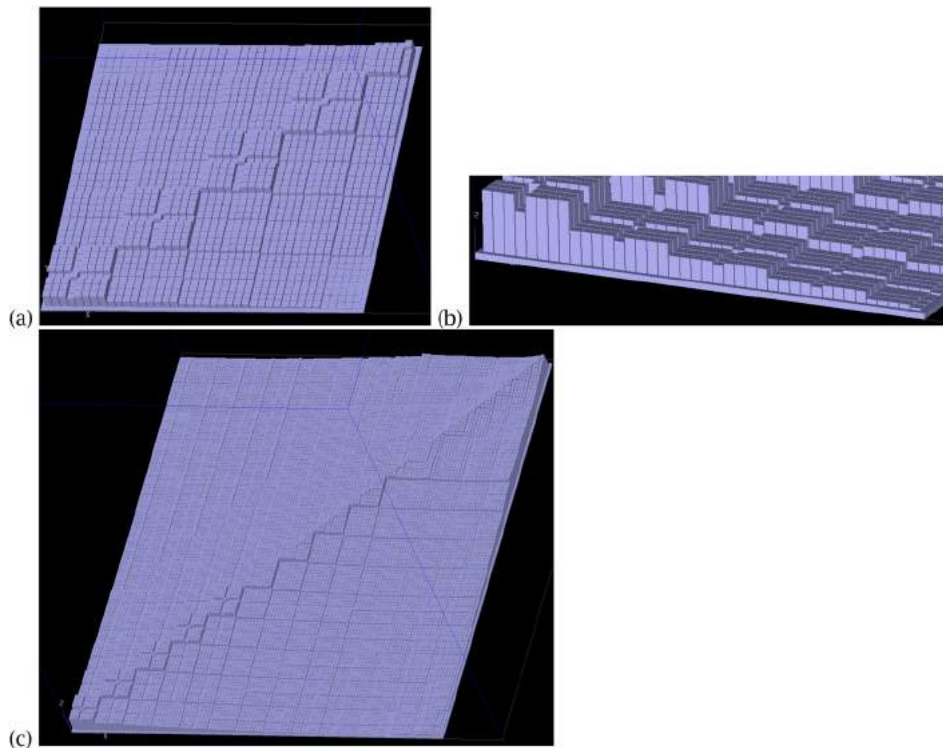
Figure 16. 3D RQ plot of a Mobius strip, embed = 10, Delay = 9, (a) Last Point = 40, (b) 4 x scale in *Z* to highlight the 'step function' type boundaries, (c) Last Point = 120.

defined bounds. This enables rapid viewing of RQ plot variants. Once the RQ plots are generated for a parameter set, a 3D model is created, as discussed in the next section.

2.1. Data acquisition: image data to sample point set

Time based data series may be extracted via various data collection methods, as done by researchers in various fields. Here, a digital image is decomposed into a flat list to represent a 'randomized' signal, as illustrated in Fig. 10. The color values employed in this analysis consist of the root mean square of the color values, which are then normalized based on the highest resultant value. For example, for a black pixel: Red = Green = Blue = 255; hence, the color value is 441, and the normalized value is 1. Two mathematical model based pictures, and two organic model based pictures are used here (Fig. 10). The two twist Mobius strip has gray scale extremes, and has a symmetric shape set as part of the model. The French curve image has interesting curvature and noise due to surface reflections. The ammonite has some symmetry although it is an organic shape, and the ginger cat image has no symmetry or obvious patterns. A sample set of the raw series input data for the Mobius strip and ginger cat is illustrated in Fig. 11. Once the RQ plots are generated

for a parameter set, a 3D model is created, as discussed in the next section.

2.2. Convert to a mesh model

The RQ plot results are converted into point geometry with position (*i, j, 0*) in Cartesian space (*XY* plane), and plotted. These points are the box center points. Bounding box objects (0.9 × 0.9 units) are created. The box is deliberately smaller than the grid size to illustrate each element. The 3D model is created by extruding the rectangles by the Euclidean norm values for each bounding box in the $+z$ direction. They joined to a base plate which has a bounding box slightly larger than the *N x N* grid, and extruded 0.25 units in the $-z$ direction. The resulting extruded surfaces are 'capped' to generate watertight models. Surface waviness is evident in the 3D RQ plots (Figs. 12 and 13).

To generate a dynamic model (variable radii representation), process planning software is employed for the FDM additive manufacturing process.

2.3. Fused deposition modeling

Fused deposition modeling is bead deposition based additive manufacturing process. AM processes are capable of fabricating three dimensional parts with
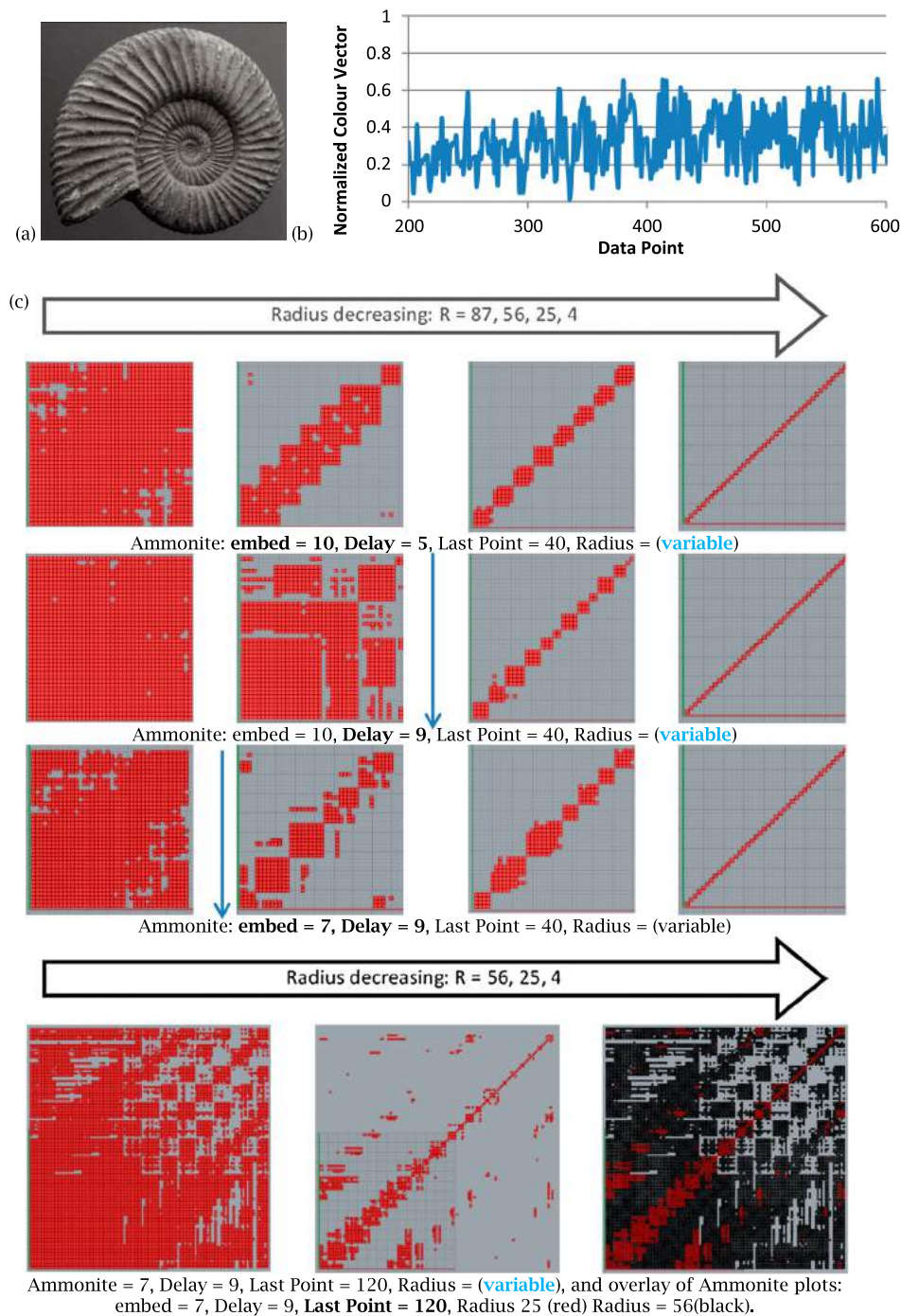
Figure 17. (a) Ammonite, (b) partial data signal, and (c) RQ plots with parameter sets as labeled showing the input variable impact.

complex geometries by layering two dimensional (2D) cross sections of build material successively to create the final part [11]. The FDM process planning software uses stereolithography files (STL) as an input, and slices into the model into layers. The slice thicknesses are predetermined, and typically vary between 0.12 to 0.33 mm. Layer visualization tools are available for process validation, as the FDM process builds a part from thin layers of molten thermoplastic filament, incorporating support material for overhanging geometry, as necessary. The contour boundaries, and fill material travel paths (raster scan pattern) are created for each slice. Consequently, for an RQ plot model, the visualization of each slice is the equivalent of viewing the neighbouring points for a threshold value, and this inherently provides a foundation for a dynamic 3D RQ plot.

Illustrated in Fig. 14 is a crude partitioned 3D model for the Mobius strip to illustrate unique data below and above a set point. This *.stl model is 33 mm high, and was sliced in 0.254 mm increments. Two selected slices – layer
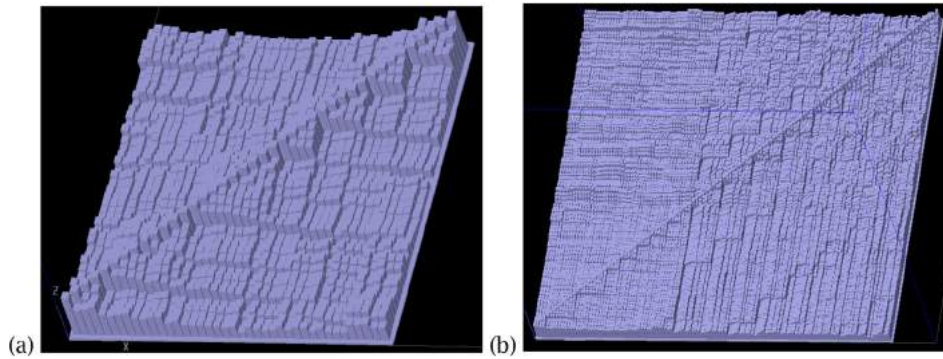
Figure 18. 3D RQ plot of the Ammonite, embed = 10, Delay = 9, (a) Last Point = 40, (b) Last Point = 120.
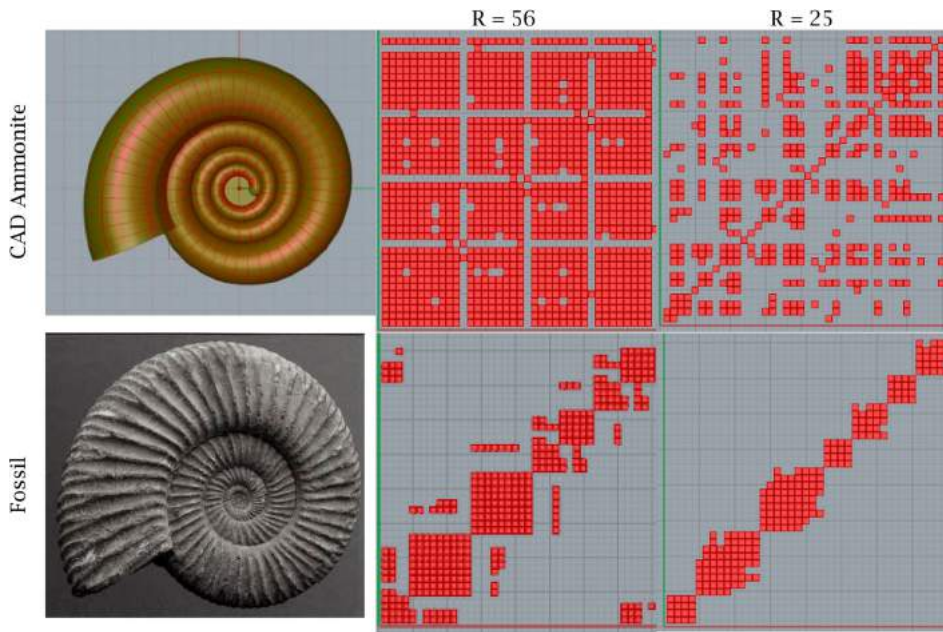
Figure 19. Ammonite input data comparisons.

51 and layer 65 for this low resolution model (Last point = 10, embed = 7, delay = 9) are shown. Note: there are 100 slices for the RQ plot area, but 130 layers total as 30 are for the base plate. At layer 25, which the equivalent of the radius = 25, a parting line is generated. Unique geometry below this radius value is extruded in the –z direction, and unique geometry extruded above this. For Fig. 14 (a), the unique geometry below the parting line (layer 55) is shown. This is constant for all layers until the parting plane is reached. Then a new set of geometry is displayed. Note: the fill pattern varies 90° between the layers; hence the different shading. The sliced layers show

3. Results

The 2D and 3D RQ plots are generated for the images for various parameter sets, as illustrated in the following figures. N is set to 40 and 120, and the other input parameters are varied to illustrate texture differences for the images. The radius is set to 87, 56, 25, and 4 as noted.

3.1. Mobius strip plots

For the four parameter sets with the various radii values, it can be seen that the Mobius strip plots have much symmetry in the RQ plot. The influence of decreasing the radius is illustrated along each row (from left to right). Changing the delay, or the data series offset, the embed value, and the total amount of data points included in the analysis is shown in Fig. 15. A 'cubic' structure is generated in both the 2D and 3D models (Fig. 15 and Fig. 16). The dynamic model for Fig. 15 (Mobius strip: embed = 7, Delay = 9, Last Point = 40) can be viewed at: http://screencast.com/t/U3whpyjr.

French curve: embed = 7, Delay = 9, Last Point = 120, Radius = (**variable**), and overlay of Ammonite plots: embed = 7, Delay = 9, **Last Point = 120**, Radius 25 (red) Radius = 56(black).

Ginger cat: embed = 7, Delay = 9, Last Point = 120, Radius = (**variable**), and overlay of Ammonite plots: embed = 7, Delay = 9, **Last Point = 120**, Radius 25 (red) Radius = 56(black).
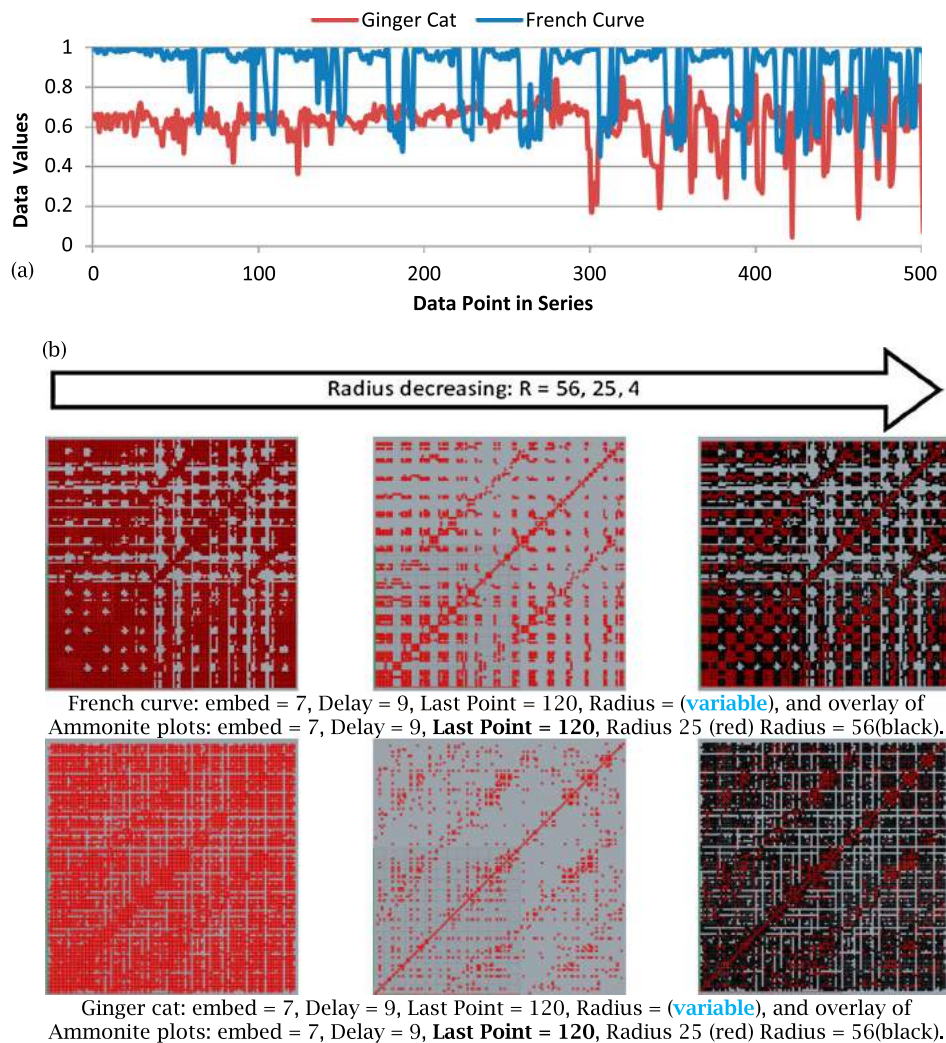
Figure 20. (a) The French curve and ginger cat data, (b) RQ plots.

3.2. Ammonite

Although the ammonite image is from an organic model, some interesting patterns with periodicity emerge (Figs. 17–18) due to the spiral pattern, and the surface ripple variations. The dynamic model for Fig. 17 (embed = 7, Delay = 9, Last Point = 40), with a 6x scaling factor in Z, can be viewed at: http://screencast.com/t/IgDStiGz25dX.

A CAD ammonite image with no surface ripples is compared to the fossil. There is little variation with the high and low radii values, so only values are R – 56 and 25 (embed = 7, Delay = 9, Last Point = 40) are plotted (Fig. 19). There are few similarities in the RQ plots although some repeatable patterns appear to be evident–the surface ripples appear to modify the input signal and RQ output significantly for the input variables chosen.

3.3. French curve and the ginger cat

The French curve has numerous curved edges, and the data series for the French curve has periodicity; whereas the ginger cat is relatively flat in the initial region as compared to the other images, and has no dominate geometric patterns in the image or the data file. The RQ plot results for both these files are busy, with dispersed patterns, as shown in Fig. 20. There is more randomness with the ginger cat RQ plot. The dynamic model for the French curve can be viewed at: http://screencast.com/t/yP5vKpYMOE7. This illustrates a comparison of two solutions (for last Point = 40, **embed = 7**, Delay = 9, and **embed = 10,** Delay = 9). For the ginger cat, a 6x scaling factor is applied in Z to emphasize the various heights. This can be viewed at: http://screencast.com/t/0n37XJGn. The
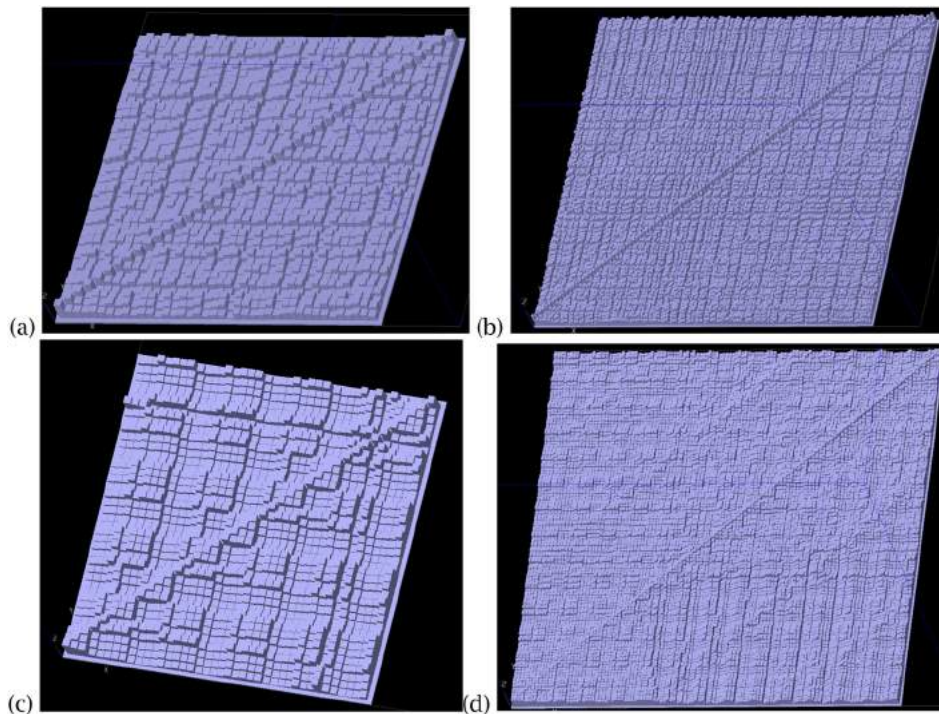
Figure 21. 3D RQ plot of a ginger cat, embed = 10, Delay = 9, (a) Last Point = 40, (b) Last Point = 120, and French curve (c) Last Point = 40, (d) Last Point = 120.

textural differences for the two images are evident in the 3D models, as shown in Fig. 21.

4. Summary

The RQ plots are generated for a set of digital image based signals, which were chosen based on their mathematical and organic shape characteristics. Once the Euclidean norm values are determined from the extracted data set, they are normalized based on their maximum value, filtered based on the selected Radius value, and then passed through the Heaviside function. A set of points is generated, which are subsequently used as a center point from which a 1.0×1.0 unit rectangular boundary is created. For the 2D plots, surfaces are created within the bounded rectangles. Parameters can be readily adjusted to visualize the results for various scenarios and images. Although this methodology allows one to vary input data and see the results dynamically, this solution does not inherently provide new insights. By introducing a normalized height vector, and extruding the 0.9×0.9 unit rectangular bounding curves by the vector height, provides a 3D model that contains all the radius values. Data can be partitioned as required, and Boolean operations can be performed to further manipulate the output results. A Boolean difference operation is performed for boxes created from offset boundary curves and cylinders generated

(a)
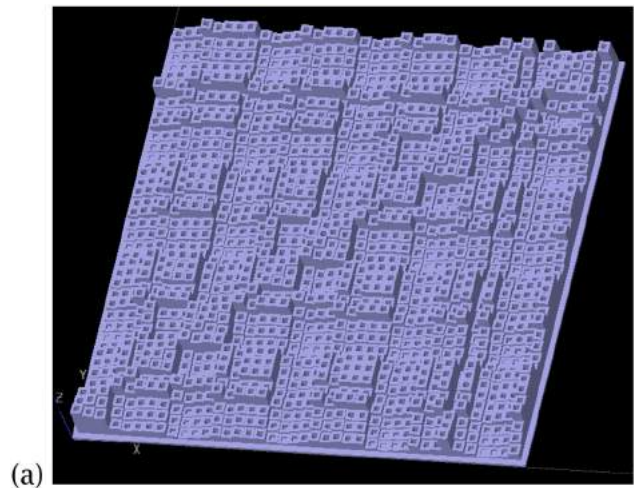
Figure 22. 3D RQ plot of the French curve employing additional Boolean operations in every cell.

around each point on the French curve 3D model, shown in Fig. 22.

The visual characteristics of the models can be modified by altering the normalizing and scaling values, as well as the parameters modified here. As a scripting language and CAD tools are utilized to implement this work, there are time lags when N is large. The build envelope for the FDM machine limits the 3D model size, and there are limitations based on the grid size. As FDM is a fabrication

technology, there are physical limitations with respect to an entity length and width, as it is assumed that beads are being deposited. The Boolean operations are time-consuming, and STL tools designed to manipulate files should be employed to extend this research. However, while working with these limitations, 3D RQ plots and dynamic models can be readily generated once the limitations of the tools are known. These models will allow for analysis and quantification approaches not available at this time.

ORCID

R. Jill Urbanic ⬤ http://orcid.org/0000-0002-2906-7618

References

[1] Acharya, U. R.; Sree, S. V.; Chattopadhyay, S.; Yu, W.; Ang, P. C. A.: Application of recurrence quantification analysis for the automated identification of epileptic EEG signals, International Journal of Neural Systems. 21(3), 2011, 199–211, https://doi.org/10.1142/S0129065711002808.

[2] Eckmann, J.P.; Kamphorst, S. O.; and Ruelle, D.: Recurrence plots of dynamical systems, Europhys. Lett. 4(9), 1987, 973–977, https://doi.org/10.1209/0295-5075/4/9/004

[3] Eneyew, E.D.; Ramulu, M.: Tool wear monitoring using microphone signals and recurrence quantification analysis when drilling composites, Advanced Materials Research. 711, 2013, 239–44, https://doi.org/10.4028/www.scientific.net/amr.711.239

[4] GhPython, McNeel, Europe software available at: http://www.food4rhino.com/project/ghpython?ufh

[5] Grasshopper 1.0, created by Scott Davidson, Lynnwood, WA, USA, software available at: http://www.grasshopper3d.com/

[6] Kantz, H.; Schreiber, T.: Nonlinear Time Series Analysis, Cambridge University Press, Cambridge, 1997.

[7] Rhinoceros 5 for Windows, Robert McNeel and Associates, Seattle WA, USA, software available at: http://www.rhino3d.com/download

[8] Stratasys Stratasys Ltd. © 2014, http://www.stratasys.com/

[9] Tahmasebpour, M.; Zarghami, R.; Sotudeh-Gharebagh, R.; Mostoufi, N.: Characterization of various structures in gas-solid fluidized beds by recurrence quantification analysis, Particuology. 11(6), 2013, 647–656.

[10] Thiel, M.; Romano, M. C.; Kurths, J.; Meucci, R.; Allaria, E.; Arecchi, F.T.: Influence of observational noise on the recurrence quantification analysis, Physica D: Nonlinear Phenomena, 171(3), 2002, 138–152, https://doi.org/10.1016/S0167-2789(02)00586-9.

[11] Townsend, V.; Urbanic, R.J.: Relating Additive and Subtractive Processes Teleologically, Rapid Prototyping Journal. 18(4), 2012, 324–338, https://doi.org/10.1108/13552541211231752.

[12] Webber, C. L.; Marwan, N.; Facchini, A.; Giuliani, A.: Simpler methods do it better: Success of Recurrence Quantification Analysis as a general purpose data analysis tool, Physics Letters A. 373(410, 2009, 3753–3756, http://doi.org/10.1016/j.physleta.2009.08.052 .

[13] Webber Jr., C.L; Zbilut, J.P.: Recurrence Quantification Analysis of Nonlinear Dynamical Systems, in Tutorials in Contemporary Nonlinear Methods for the Behavioral Sciences, M. A. Riley, G. C. Van Orden, eds. National Science Foundation (U.S.), 2005, 26–94. http://www.nsf.gov/sbe/bcs/pac/nmbs/nmbs.pdf

[14] Zbilut, J.P.; Webber Jr., C.L.: Dynamical assessment of physiological systems and states using recurrence plot strategies, Journal of Applied Physiology. 76(2), 1994, 965–973.

[15] Zbilut, J.P.; Webber Jr., C.L.: Embeddings and delays as derived from quantification of recurrence plots, Physics Letters A. 171(3–4), 1992, 199–203, https://doi.org/10.1016/0375-9601(92)90426-M.

[16] Zhao, Z.Q.; Li, S.C.; Gao, J.B.; Wang, Y.L.: Identifying spatial patterns and dynamics of climate change using recurrence quantification analysis: A case study of qing-haitibet plateau, International Journal of Bifurcation and Chaos. 21(4), 2011, 1127–1139, https://doi.org/10.1142/S0218127411028933.